

## Sonochemical Fabrication and Photoluminescence Properties of Ordered Mesoporous Carbon–Tin Oxide Nanocomposites

Yulin Cao, Jieming Cao,\* Jinsong Liu, Mingbo Zheng, and Kai Shen  
*Nanomaterials Research Institute, College of Material Science and Technology,  
Nanjing University of Aeronautics and Astronautics, Nanjing 210016, P. R. China*

(Received September 22, 2006; CL-061103; E-mail: jmcao@nuaa.edu.cn)

A new ordered mesoporous carbon–tin oxide (OMC–SnO<sub>2</sub>) nanocomposite has been prepared for the first time by a simple and efficient sonochemical route at room temperature. The resulting SnO<sub>2</sub> nanoparticles are about 3 nm in size and highly dispersed on ordered mesoporous carbon. The photoluminescence properties of the OMC–SnO<sub>2</sub> composites are also firstly described. This method is proposed as a simple and general method to prepare new functionalized ordered mesoporous carbon materials with other nanoparticles for various applications.

Ordered mesoporous carbons (OMCs) with different structures prepared from various silica templates and carbon precursors are of great interest because these materials are useful for catalyst supports, absorbents, hydrogen storage media, and advanced electrodes.<sup>1</sup> To generate new use of OMCs in various applications, it is useful to attach functional nanoparticles to their surface. Several metal or metal oxide nanoparticles, such as Pt, Pd, Sn, NiO, MnO<sub>2</sub>, Fe<sub>2</sub>O<sub>3</sub>, etc., have been inserted into the mesostructure of OMCs.<sup>2</sup>

Tin oxide (SnO<sub>2</sub>) is an important n-type semiconductor with a wide energy gap because of its wide applications in conductive electrodes, heterojunction solar cells, and chemical sensors. SnO<sub>2</sub> deposited on carbon nanotubes (CNTs) has been used for a new hybrid gas sensor and solves a problem of conventional SnO<sub>2</sub> sensors that are not able to detect NO<sub>2</sub> gas at room temperature.<sup>3</sup> Compared with CNTs, OMCs possess high surface area, large pore volume, excellent mechanic stability, and electrical conductivity, which could serve as inert, high surface area nanoscale scaffolds on which functional nanosized particles are attached. However, to the best of our knowledge, there are no reports on the fabrication of OMC–SnO<sub>2</sub> nanocomposites. Hence, it is still a challenge to explore a simple and efficient route for controllably coating OMCs with inorganic materials.

Here, we report the first fabrication of OMC–SnO<sub>2</sub> nanocomposites by a simple and efficient sonochemical route under ambient air. SnCl<sub>4</sub> is used as a precursor to coat OMCs fully with uniform and highly dispersed SnO<sub>2</sub> nanoparticle. Mesoporous SBA-15 silica and ordered CMK-3 mesoporous carbon were prepared according to the literature procedures.<sup>4</sup> In a typical procedure, 1.0 g of tin chloride was dispersed in 50 mL of distilled H<sub>2</sub>O, followed by addition of 0.8 mL of HCl (38%). After the addition of 20 mg of CMK-3, this solution was sonicated for 30 min and then stirred for 4 h at room temperature. The treated sample was then rinsed with distilled H<sub>2</sub>O. The final products were denoted as OMC–SnO<sub>2</sub>.

Products were characterized by X-ray diffraction (XRD) (Bruker D8-Advance), transmission electron microscopy (TEM) (FEI TECNAI-20), N<sub>2</sub> adsorption/desorption measurement (Micromeritics ASAP 2010 system), and scanning electron

microscopy (SEM) (LEO1530). The room-temperature photoluminescence (PL) spectra were measured using a Hitachi M-850 fluorescence spectrometer under an excitation of 398 nm.

Figure S1a<sup>9</sup> shows the low-angle XRD patterns of SBA-15 and CMK-3. Both SBA-15 and CMK-3 samples show three resolved peaks that can be basically indexed as (100), (110), and (200) reflections associated with the 2-D hexagonal *P6mm* symmetry, indicating the ordered arrangement of the nanopores in these samples. Figure S1b<sup>9</sup> shows the wide-angle XRD patterns of the OMC–SnO<sub>2</sub> composites. All the diffraction lines are assigned well to tetragonal rutile crystalline phases of tin oxide with a reference pattern (JCPDS 41-1445). The broadening of SnO<sub>2</sub> peaks in the XRD pattern is due to the small particle size. The average particle size of the deposited SnO<sub>2</sub> particles is estimated as 3.3 nm calculated from the Scherrer equation.

Figure 1 shows the TEM images of CMK-3 and OMC–SnO<sub>2</sub> recorded perpendicular to the mesoporous orientation (also shown in Figure S2<sup>9</sup>). Figure 1a shows that the carbon nanorods in CMK-3 are 7 nm in diameter and the center-to-center distances of adjacent channels are about 10 nm. A high degree of uniform nanoparticles immobilization can be observed on the surface of the CMK-3 shown in Figure 1b. Figure 1c shows that the SnO<sub>2</sub> nanoparticles are ultrafine and the particle size of these nanoparticles is about 3 nm, which is coincident with the size of particles calculated from the Scherrer equation. The chemical composition of OMC–SnO<sub>2</sub> was investigated by energy-dispersive X-ray spectroscopy (EDS). EDS shown in Figure S2<sup>9</sup> confirms the presence of Sn, O, C, and Cu in the coated CMK-3. The elements Sn and O originate from the SnO<sub>2</sub> nanoparticles. In addition, the existence of C in the EDS spectrum results mostly from CMK-3 host and partially from the carbon film on copper grid. The Cu peaks originate from the copper grid.

Figure S3<sup>9</sup> shows N<sub>2</sub> adsorption–desorption isotherms of SBA-15, CMK-3, and OMC–SnO<sub>2</sub>, and the pore size distribution curves obtained from the adsorption branch and the data are listed in Table S1.<sup>9</sup> N<sub>2</sub> adsorption–desorption isotherms of both SBA-15 and CMK-3 samples yield H1-type hysteresis that is typical of mesoporous materials with 1-D cylindrical chan-

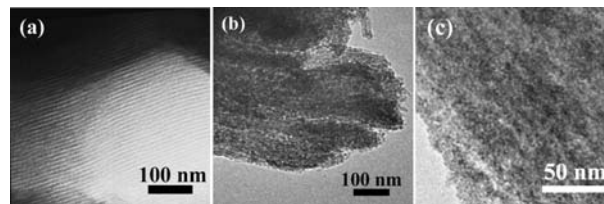


**Figure 1.** Typical TEM images of (a) CMK-3, and (b) the OMC–SnO<sub>2</sub> material recorded perpendicular to the mesoporous orientation. (c) TEM image (higher magnification) of the OMC–SnO<sub>2</sub> materials.

nels. Pore size distribution of SBA-15 is centered at 9.3 nm. The BET surface area and pore volume of the SBA-15 silica are  $580 \text{ m}^2 \text{ g}^{-1}$  and  $1.02 \text{ cm}^3 \text{ g}^{-1}$ , respectively. CMK-3 has a BET surface area of  $1189 \text{ m}^2 \text{ g}^{-1}$ , a pore volume of  $1.35 \text{ cm}^3 \text{ g}^{-1}$ , and a pore size distribution of 4.3 nm. For the OMC-SnO<sub>2</sub> composites, N<sub>2</sub> adsorption measurement shows a reduced capillary filling step due to the deposition of SnO<sub>2</sub> nanoparticles on CMK-3. The pore size distribution of OMC-SnO<sub>2</sub> is mainly located at 2–5 nm, and the average pore size calculated by BJH algorithm is 3.5 nm. The BET surface area and pore volume of OMC-SnO<sub>2</sub> are  $646 \text{ m}^2 \text{ g}^{-1}$  and  $0.47 \text{ cm}^3 \text{ g}^{-1}$ , respectively. The OMC-SnO<sub>2</sub> nanocomposites still have a large BET surface area, which may be useful for potential application in chemical sensor.

The changes in surface morphology for the modified samples were also investigated with a scanning electron microscope (SEM). The unmodified CMK-3 carbon shows a clean surface shown in Figure S4a.<sup>9</sup> The primary distance between carbon nanorods in CMK-3 is estimated as 10 nm, which can be clearly observed in Figure S4b.<sup>9</sup> Figure S4c<sup>9</sup> shows a SEM image of the modified OMC-SnO<sub>2</sub> sample. The chemical attachment of functionalized SnO<sub>2</sub> nanoparticles on the carbon surface increases the surface roughness.

To investigate the electronic properties of the functionalized OMC-SnO<sub>2</sub> composites, room-temperature photoluminescence (PL) experiments were also firstly performed. The emission spectrum shown in Figure 2 presents two bands at 418 and 544 nm, respectively. The broad yellow bands (544 nm) in the spectra can be attributed to oxygen vacancies, which act as deep defect donors in semiconductor oxides and would form a series of meta-stable energy levels within the band gap of SnO<sub>2</sub>.<sup>5</sup> The origins of the blue/violet bands (418 nm) maybe are related to structural defects.<sup>6</sup> On the whole, the sonochemical method may give high-quality crystals with low defect densities, which further results in visual emissions.

A mechanism is proposed to account for the fabrication of SnO<sub>2</sub> nanoparticles supported on ordered mesoporous carbon. It is well known that ultrasonic irradiation of liquids has a variety of physical and chemical effects derived from acoustic cavitation and can provide a unique method for driving chemical reactions under extreme conditions.<sup>7</sup> Sonochemistry has already been used for the insertion of various species, such as Co/Mo oxide, WS<sub>2</sub>, MoS<sub>2</sub>, and noble metal into the mesoporous silica materials.<sup>8</sup> Sonication of the precursor in the presence of a host material provides an alternative means of trapping the produced nanoparticles, which has been used in this work to produce the OMC-SnO<sub>2</sub> nanocomposites. The formation of SnO<sub>2</sub> is presented as  $2\text{SnCl}_2 + 2\text{H}_2\text{O} + \text{O}_2 \rightarrow 2\text{SnO}_2 + 4\text{HCl}$ . The generated SnO<sub>2</sub> nanoclusters can deposit on the mesoporous carbon carriers in the solution and form a SnO<sub>2</sub>-capped mesoporous carbon

composite, which is termed as an OMC-SnO<sub>2</sub> nanocomposite in this work. The sonochemical method is advantageous as it is simple, nonhazardous, rapid in reaction rate and produces very small metal oxide particles. We anticipate that the SnO<sub>2</sub> thin coating with ultrafine SnO<sub>2</sub> nanoparticles produced in the present work will exhibit interesting chemical and physical properties relevant to technological applications. We also note our coating method is not restricted only to OMC and SnO<sub>2</sub> nanoparticles. We believe that this method can be generally used to coat OMCs with other substances by selecting different chlorides for this reaction.

In conclusion, for the first time, the SnO<sub>2</sub> nanoparticle-functionalized ordered mesoporous carbon nanocomposites have been successfully prepared through a simple sonochemical method at room temperature. The resulting SnO<sub>2</sub> nanoparticles are about 3 nm and highly dispersed on ordered mesoporous carbon. The optical properties may also be of significant interest due to the prominent variations in the electronic structure of the constituting phases. This method is also proposed as a simple and general method to prepare new functionalized ordered mesoporous carbon materials with other nanoparticles for various applications in catalysis, adsorption, sensor, and nanoelectronic device.

Financial supports from the National Natural Science Foundation of China (No. 50502020) and Natural Science Foundation of Jiangsu Province (BK2006195) are gratefully acknowledged.

## References and Notes

- a) G. S. Chai, S. B. Yoon, J. S. Yu, J. H. Choi, Y. E. Sung, *J. Phys. Chem. B* **2004**, *108*, 7074. b) A. Vinu, C. Streb, V. Murugesan, M. Hartmann, *J. Phys. Chem. B* **2003**, *107*, 8297. c) J. B. Pang, J. E. Hampsey, Z. W. Wu, Q. Y. Hu, Y. F. Lua, *Appl. Phys. Lett.* **2004**, *85*, 4887. d) H. S. Zhou, S. M. Zhu, M. Hibino, I. Honma, M. Ichihara, *Adv. Mater.* **2003**, *15*, 2107. e) R. Ryoo, S. H. Joo, M. Kruk, M. Jaroniec, *Adv. Mater.* **2001**, *13*, 677.
- a) S. H. Joo, S. J. Choi, I. Oh, J. Kwak, Z. Liu, O. Terasaki, R. Ryoo, *Nature* **2001**, *412*, 169. b) É. Sípós, G. Fogassy, A. Tungler, P. V. Samant, J. L. Figueiredo, *J. Mol. Catal. A: Chem.* **2004**, *212*, 245. c) I. Grigoriants, L. Sominski, H. L. Li, I. Ifargan, D. Aurbach, A. Gedanken, *Chem. Commun.* **2005**, 921. d) H. Li, S. Zhu, H. Xi, R. Wang, *Microporous Mesoporous Mater.* **2006**, *89*, 196. e) S. Zhu, H. Zhou, M. Hibino, I. Honma, M. Ichihara, *Adv. Funct. Mater.* **2005**, *15*, 381. f) H. Huwe, M. Fröba, *Microporous Mesoporous Mater.* **2003**, *60*, 151.
- Y. X. Liang, Y. J. Chen, T. H. Wang, *Appl. Phys. Lett.* **2004**, *85*, 666.
- a) D. Zhao, J. Feng, Q. Huo, N. Melosh, G. H. Fredrickson, B. F. Chmelka, G. D. Stucky, *Science* **1998**, *279*, 548. b) S. Jun, S. H. Joo, R. Ryoo, M. Kruk, M. Jaroniec, Z. Liu, T. Ohsuna, O. Terasaki, *J. Am. Chem. Soc.* **2000**, *122*, 10712.
- Y. S. He, J. C. Campbell, R. C. Murphey, N. F. Arendt, J. S. Swinnea, *J. Electron. Mater.* **1993**, *8*, 3131.
- T. W. Kim, D. U. Lee, Y. S. Yoon, *J. Appl. Phys.* **2000**, *88*, 3759.
- K. S. Suslick, G. J. Price, *Annu. Rev. Mater. Sci.* **1999**, *29*, 295.
- a) A. Gedanken, X. Tang, Y. Wang, N. Perkash, Y. Koltypin, M. V. Landau, L. Vradman, M. Herskowitz, *Chem. Eur. J.* **2001**, *7*, 4546. b) L. Vradman, M. V. Landau, M. Herskowitz, V. Ezersky, M. Talianker, S. Nikitenko, Y. Koltypin, A. Gedanken, *J. Catal.* **2003**, *213*, 163. c) L. Vradman, M. V. Landau, M. Herskowitz, V. Ezersky, M. Talianker, S. Nikitenko, Y. Koltypin, A. Gedanken, *Stud. Surf. Sci. Catal.* **2003**, *146*, 721. d) W. Chen, W. P. Cai, Z. P. Zhang, L. Zhang, *Chem. Lett.* **2001**, 152.
- Supporting Information is available electronically on the CSJ-Journal web site <http://www.csj.jp/journals/chem-lett/index.html>.

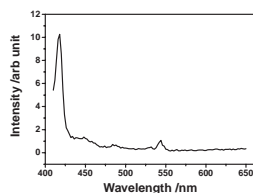


**Figure 2.** Room temperature PL spectra of the OMC-SnO<sub>2</sub> materials.